Chapter 10
Single Track Models

Single track models allow a physically plausible description of the driving behavior of vehicles without major modeling and parameterization effort. Hence, in this chapter a number of linear and nonlinear single track models will be described.

10.1 Linear Single Track Model

The classic linear single track model (Riekert and Schunk 1940) allows the approximate, yet physically plausible description of the lateral dynamics of a vehicle, Ref. (Fig. 10.1).
The modeling is based on a series of simplifications:

- The velocity of the vehicle's center of gravity is considered to be constant along the longitude of its trajectory.
- All lifting, rolling and pitching motion will be neglected.
- The vehicle's mass is assumed to be concentrated at the center of gravity S.
- The front and the rear tires will be represented as one single tire on each axle. The imaginary tire contact points V and H, which the tire forces are to act upon, lie along the center of the axle.
- The pneumatic trail and the aligning torque resulting from the slip angle of the tire will be neglected.
- The wheel-load distribution between front and rear axle is assumed to be constant.
- The longitudinal forces on the tires, resulting from the assumption of a constant longitudinal velocity, will be neglected.

The first two assumptions lead to four constraints for the six degrees of freedom of rigid bodies in the model. As a result, the only possible motion left is the heading angle (yaw angle) ψ_V, which only occurs in the form of the yaw rate $\dot{\psi}_V$, and the side slip angle β. The side slip angle represents the direction of the deviation of the center of gravity from the vehicle's steering axis. The steering angle δ of the front

D. Schramm et al., *Vehicle Dynamics*, DOI: 10.1007/978-3-540-36045-2_10,

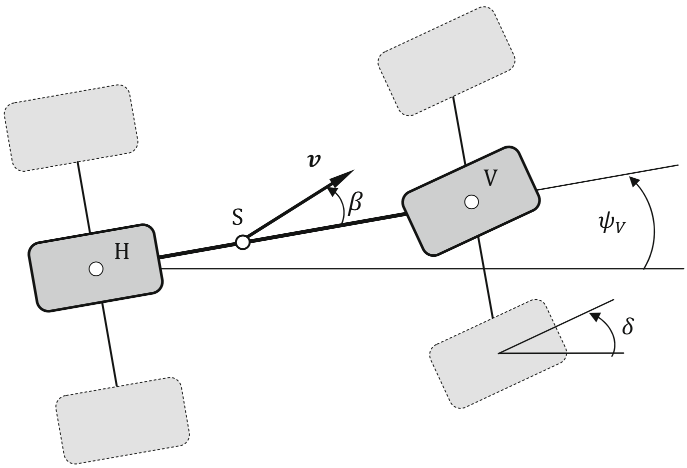

Fig. 10.1 Linear single track model

axle serves as the input parameter. This greatly idealized vehicle model allows the investigation of the fundamental driving dynamic relationships within the lateral acceleration region of

$$a_y \leq 0,4g \approx 4\,\frac{\mathrm{m}}{\mathrm{s}^2} \tag{10.1}$$

on dry roads (Ammon 2013).

10.1.1 Equations of Motion of the Linear Single Track Model

To generate the equations of motion the rigid body kinematics of the vehicle has to be reviewed. To this end, the kinematics of the vehicle in the x_E, y_E-plane of the inertial system can be described as $\mathbf{K}_E = \{\mathrm{O}_E; x_E, y_E, z_E\}$, Ref. Fig. 10.2. Especially in the quasi-stationary situation, i.e. for very small velocities $\boldsymbol{v}$ of the center of gravity S, all points of the vehicle move along a circle with the center of the curvature being K_A. In this case, this coincides with the instantaneous center of rotation M of the motion. The steering angle required to execute this motion is, under the assumption of small steering motion and large radii of curvature relative to the measurements of the vehicle, given as:

$$\tan\delta_A = \frac{l}{\sqrt{\rho_M^2 - l_h^2}} \xrightarrow{|\delta_A| \ll 1,\, l_h \ll \rho_M} \delta_A \approx \frac{l}{\rho_M}. \tag{10.2}$$

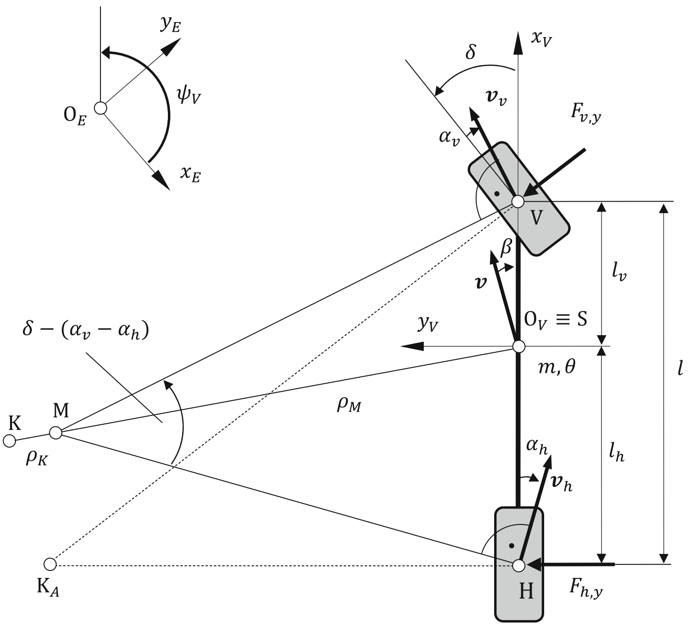

Fig. 10.2 Mathematical description of the linear single track model

The steering angle δ_A of the front wheels resulting from Eq. (10.2) is called the Ackermann steering angle.

In general, the vehicle velocity is given according to (Fig. 10.2) in the vehicle fixed coordinate system $\mathbf{K}_V = \{O_V; x_V, y_V, z_V\}$:

$$ {}^V\boldsymbol{v} = \begin{bmatrix} v\cos\beta \\ v\sin\beta \\ 0 \end{bmatrix}. \tag{10.3}$$

The acceleration of the vehicle's center of gravity S, represented in the coordinate system $\mathbf{K}_V$, is therefore:

$$\begin{aligned} {}^V\boldsymbol{a} &= \frac{d\,{}^V\boldsymbol{v}}{dt} + {}^V\boldsymbol{\omega} \times {}^V\boldsymbol{v} = \begin{bmatrix} -v\sin\beta\dot{\beta} \\ v\cos\beta\dot{\beta} \\ 0 \end{bmatrix} + \begin{bmatrix} 0 \\ 0 \\ \dot{\psi}_V \end{bmatrix} \times \begin{bmatrix} v\cos\beta \\ v\sin\beta \\ 0 \end{bmatrix} \\ &= \begin{bmatrix} -v\left(\dot{\psi}_V + \dot{\beta}\right)\sin\beta \\ v\left(\dot{\psi}_V + \dot{\beta}\right)\cos\beta \\ 0 \end{bmatrix}. \end{aligned} \tag{10.4}$$

Due to the assumption of a constant longitudinal velocity $v = const$, the acceleration $\boldsymbol{a}$ is only a purely normal acceleration $\boldsymbol{a}_n$, perpendicular to the vehicle ($\boldsymbol{a}^T\boldsymbol{v} = 0$). Its magnitude is given by:

$$a_n = |\boldsymbol{a}_n| = v\left(\dot{\psi}_V + \dot{\beta}\right). \tag{10.5}$$

From Fig. 10.2 it can be inferred that the radius of curvature ρ_K of the path curve of the center of gravity is described by

$$\rho_K = \frac{v}{\left(\dot{\psi}_V + \dot{\beta}\right)}. \tag{10.6}$$

For the following observations, the acceleration of the center of gravity perpendicular to the vehicle velocity is required. For small side slip angles β according to Eq. (10.6), this results in:

$$a_y = v\left(\dot{\psi}_V + \dot{\beta}\right)\cos\beta \approx v\left(\dot{\psi}_V + \dot{\beta}\right) = \frac{v^2}{\rho_K}. \tag{10.7}$$

The calculation of the horizontal tire forces still requires the velocities of the tire contact point. These are calculated according to Fig. 10.2:

$$\begin{aligned} {}^V\boldsymbol{v}_v &= {}^V\boldsymbol{v} + {}^V\boldsymbol{\omega} \times {}^V_S\boldsymbol{r}_V \\ &= \begin{bmatrix} v\cos\beta \\ v\sin\beta \\ 0 \end{bmatrix} + \begin{bmatrix} 0 \\ 0 \\ \dot{\psi} \end{bmatrix} \times \begin{bmatrix} l_v \\ 0 \\ 0 \end{bmatrix} = \begin{bmatrix} v\cos\beta \\ v\sin\beta + l_v\dot{\psi}_V \\ 0 \end{bmatrix}, \end{aligned} \tag{10.8}$$

at the front wheels and

$$\begin{aligned} {}^V\boldsymbol{v}_h &= {}^V\boldsymbol{v} + \boldsymbol{\omega} \times {}^V_S\boldsymbol{r}_h \\ &= \begin{bmatrix} v\cos\beta \\ v\sin\beta \\ 0 \end{bmatrix} + \begin{bmatrix} 0 \\ 0 \\ \dot{\psi}_V \end{bmatrix} \times \begin{bmatrix} -l_h \\ 0 \\ 0 \end{bmatrix} = \begin{bmatrix} v\cos\beta \\ v\sin\beta - l_h\dot{\psi}_V \\ 0 \end{bmatrix} \end{aligned} \tag{10.9}$$

at the rear wheels. Here, ${}_S\boldsymbol{r}_v$ and ${}_S\boldsymbol{r}_h$ are the position vectors based on the center of gravity S of the vehicle to the front tire contact point V and to the rear contact point H respectively. The current velocity $\boldsymbol{v}_v$ of the front wheels can now be expressed as the side slip angle β and the steering angle δ in the vehicle fixed coordinate system $\mathbf{K}_V$:

$${}^V\boldsymbol{v}_v = \begin{bmatrix} v\cos\beta \\ v\sin\beta + l_v\dot{\psi}_V \\ 0 \end{bmatrix} = \begin{bmatrix} v_v\cos(\delta - \alpha_v) \\ v_v\sin(\delta - \alpha_v) \\ 0 \end{bmatrix}. \tag{10.10}$$

Fig. 10.3 Tire loads in a linear single track model

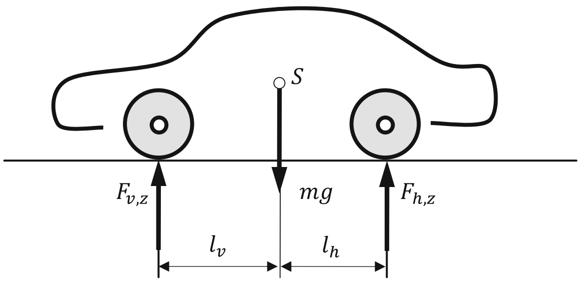

The first two components in Eq. (10.10) offer the relationship to the front slip angle α_v for small steering angles δ:

$$\begin{aligned} \tan(\delta - \alpha_v) &= \frac{v \sin\beta + l_v \dot{\psi}_V}{v \cos\beta} \approx \beta + l_v \frac{\dot{\psi}_V}{v} \\ \Rightarrow \alpha_v &= \delta - \beta - l_v \frac{\dot{\psi}_V}{v}. \end{aligned} \tag{10.11}$$

This procedure can be applied similarly to the rear axle:

$$^V\boldsymbol{v}_h = \begin{bmatrix} v \cos\beta \\ v \sin\beta - l_h \dot{\psi}_V \\ 0 \end{bmatrix} = \begin{bmatrix} v_h \cos\alpha_h \\ -v_h \sin\alpha_h \\ 0 \end{bmatrix}. \tag{10.12}$$

From the first and the second components of this vector equation, one then gets:

$$\begin{aligned} -\tan\alpha_h &= \frac{v \sin\beta - l_h \dot{\psi}}{v \cos\beta} \approx \beta - l_h \frac{\dot{\psi}_V}{v}, \\ \Rightarrow \alpha_h &\approx -\beta + l_h \frac{\dot{\psi}_V}{v}. \end{aligned} \tag{10.13}$$

To set up the equations of motion, the values of the forces acting on the vehicle along with the kinematic descriptions are still required. While still considering the position of the center of gravity of the vehicle (Fig. 10.3), the normal forces on the tires are given by:

$$F_{v,z} = mg \frac{l_h}{l} \quad \text{and} \quad F_{h,z} = mg \frac{l_v}{l}. \tag{10.14}$$

The tire forces may then be calculated assuming a linear relationship between the lateral forces and the tire slip angles as discussed in Chap. 7:

$$F_{v,y} = c_{\alpha,v}\, \alpha_v \quad \text{and} \quad F_{h,y} = c_{\alpha,h}\, \alpha_h, \tag{10.15}$$

with the cornering stiffnesses $c_{\alpha,v}$ and $c_{\alpha,h}$ (Ref. Fig. 10.4).

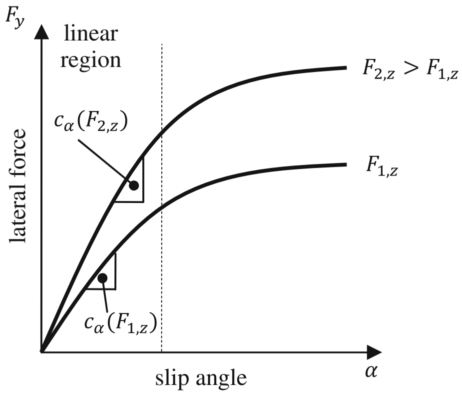

Fig. 10.4 Relationship between the tire lateral forces and the slip angle

In Fig. 10.4 it is noteworthy that the cornering stiffness is a function of the tire loads. This will be dealt with in more detail in Sect. 10.3. With help of the accelerations (10.4) and Fig. 10.4, the principle of linear momentum in the lateral direction yields

$$mv\left(\dot{\psi}_V + \dot{\beta}\right)\cos\beta = \cos\delta\, F_{v,y} + F_{h,y}. \tag{10.16}$$

The corresponding principle of angular momentum about the vertical axis is

$$\theta\ddot{\psi}_V = F_{v,y}\cos\delta\, l_v - F_{h,y}\, l_h. \tag{10.17}$$

If one were to substitute the expressions for the tire's lateral forces with the relationships given in Eq. (10.15) as well as in Eqs. (10.11) and (10.13) and considering $\cos\beta \approx 1, \cos\delta \approx 1$ for $|\beta|, |\delta| \ll 1$, one finally arrives at the two equations of motion of the linear single track model:

$$mv\dot{\beta} + \left(mv^2 + c_{\alpha,v}l_v - c_{\alpha,h}l_h\right)\frac{\dot{\psi}_V}{v} + \left(c_{\alpha,v} + c_{\alpha,h}\right)\beta = c_{\alpha,v}\delta, \tag{10.18}$$

$$\theta\ddot{\psi}_V + \left(c_{\alpha,v}l_v^2 + c_{\alpha,h}l_h^2\right)\frac{\dot{\psi}_V}{v} + \left(c_{\alpha,v}l_v - c_{\alpha,h}l_h\right)\beta = c_{\alpha,v}l_v\delta. \tag{10.19}$$

With the substitution

$$\boldsymbol{x} = \begin{bmatrix} x_1 \\ x_2 \end{bmatrix} = \begin{bmatrix} \dot{\psi}_V \\ \beta \end{bmatrix}, \tag{10.20}$$

one arrives at the state space representation

$$\underbrace{\begin{bmatrix} \dot{x}_1 \\ \dot{x}_2 \end{bmatrix}}_{\dot{\boldsymbol{x}}} = \underbrace{\begin{bmatrix} -\frac{1}{v}\frac{c_{\alpha,v}l_v^2 + c_{\alpha,h}l_h^2}{\theta} & -\frac{c_{\alpha,v}l_v - c_{\alpha,h}l_h}{\theta} \\ -1 - \frac{1}{v^2}\frac{c_{\alpha,v}l_v - c_{\alpha,h}l_h}{m} & -\frac{1}{v}\frac{c_{\alpha,v} + c_{\alpha,h}}{m} \end{bmatrix}}_{\boldsymbol{A}} \underbrace{\begin{bmatrix} x_1 \\ x_2 \end{bmatrix}}_{\boldsymbol{x}} + \underbrace{\begin{bmatrix} \frac{c_{\alpha,v}l_v}{\theta} \\ \frac{1}{v}\frac{c_{\alpha,v}}{m} \end{bmatrix}}_{\boldsymbol{B}} \underbrace{[\delta]}_{\boldsymbol{u}} \tag{10.21}$$

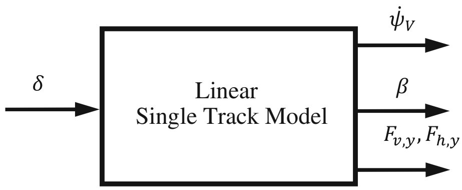

Fig. 10.5 Linear single track model as a dynamic system

with the [2 × 1]-state vector $\boldsymbol{x}$, the [2 × 2]-system matrix $\boldsymbol{A}$, the [2 × 1]-control matrix $\boldsymbol{B}$ and the [1 × 1]-input vector $\boldsymbol{u}$. This leads to the representation of the linear single track model as a dynamic system with a corresponding transfer function (Fig. 10.5). The representation (10.21) is a suitable basis for fundamental analysis of vehicle dynamics. This will be exemplified in the following sections. For a more detailed analysis, the interested reader is referred to (Willumeit 1998).

10.1.2 Stationary Steering Behavior and Cornering

For cornering along a circle with a constant radius ρ, the steering angle δ as well as the yaw rate $\dot{\psi}_V$ and the side slip angle β are all constant, i.e. it follows:

$$\delta = const, \dot{\delta} = 0, \tag{10.22}$$

$$\dot{\psi}_V = const, \ddot{\psi}_V = 0, \tag{10.23}$$

$$\beta = const, \dot{\beta} = 0, \tag{10.24}$$

$$\rho_K = \frac{v}{\dot{\psi}_V + \dot{\beta}} = \frac{v}{\dot{\psi}_V} = \rho. \tag{10.25}$$

With the additional constraints (10.22)–(10.25) and by implementing the Eqs. (10.16) and (10.17) as well as considering the Eq. (10.15), in a single step one obtains the relationship:

$$\alpha_v - \alpha_h = \frac{mv^2}{\rho l}\left(\frac{l_h}{c_{\alpha,v}} - \frac{l_v}{c_{\alpha,h}}\right) = \underbrace{\frac{m}{l}\left(\frac{l_h c_{\alpha,h} - l_v c_{\alpha,v}}{c_{\alpha,v} c_{\alpha,h}}\right)}_{EG}\frac{v^2}{\rho}. \tag{10.26}$$

The expression EG in Eq. (10.26) is called the self-steering gradient which characterizes the typical driving behavior of a given vehicle for a given steering motion. As a result, one can for example solve the following practical problems:

- Which steering angle $\delta_H = i_L \delta$ with the steering transmission ratio i_L is necessary for a vehicle with a velocity v to follow a circle with a radius ρ?

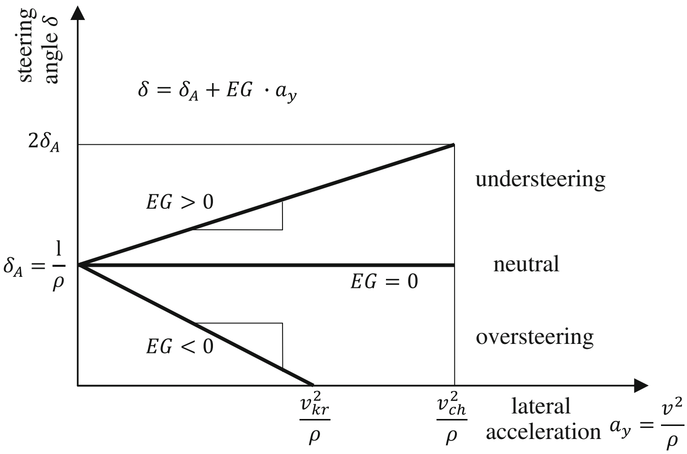

Fig. 10.6 Self steering gradient in the linear region

- Which parameters become stationary when a steering angle δ_H is applied to a vehicle travelling in a straight line?
- What happens in the transition region (instationary steering behavior)?

To answer the first question, one first calculates the slip angle and the steering angle for a given circle with the radius ρ. From the side slip angle of the rear wheels (10.13), the side slip angle of the vehicle can be calculated using the transformation:

$$\beta = l_h \frac{\dot{\psi}_V}{v} - \alpha_h = \frac{l_h}{\rho} - \frac{m}{c_{\alpha,h}} \frac{l_v}{l} \frac{v^2}{\rho}. \tag{10.27}$$

The steering angle required for the circular path is then given with the slip angle at the front wheels (10.11):

$$\begin{aligned} \delta &= l_v \frac{\dot{\psi}_V}{v} + \alpha_v + \beta = \frac{l}{\rho} + \alpha_v - \alpha_h \\ &= \underbrace{\frac{l}{\rho}}_{\delta_A} + \underbrace{\frac{m}{l} \left(\frac{l_h c_{\alpha,h} - l_v c_{\alpha,v}}{c_{\alpha,v} c_{\alpha,h}} \right)}_{EG} \underbrace{\frac{v^2}{\rho}}_{a_y} = \delta_A + EG \cdot a_y. \end{aligned} \tag{10.28}$$

The first summand occurring in Eq. (10.28) is the Ackermann steering angle (compare Eq. (10.2)). With increasing velocity v, the required steering angle increases or decreases for a given circular path, depending on the sign of the self-steering gradient EG, Ref. (Fig. 10.6). If the required steering angle is greater than the Ackermann steering angle ($EG > 0$), this is called under steering driving behavior, in the case of ($EG < 0$), it is called over steering driving behavior. In case of $EG = 0$, it is characterized as a neutral driving behavior.

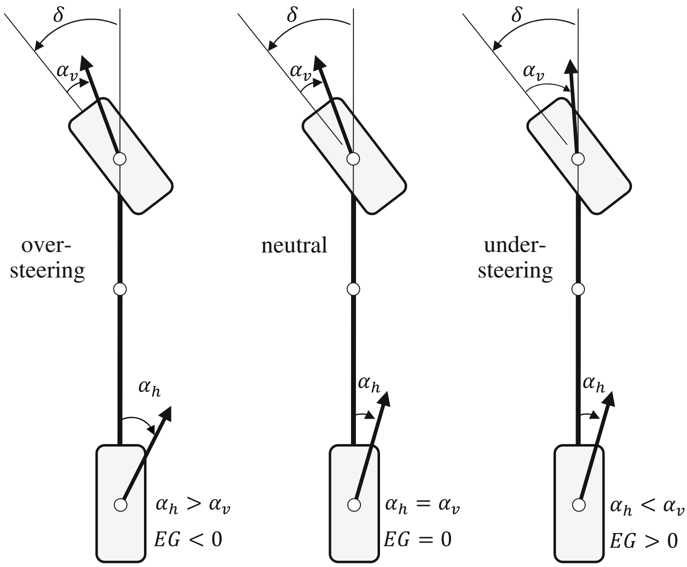

Fig. 10.7 Self-steering behavior of a linear single track model

From Eq. (10.28), one can also derive the relationship

$$EG \cdot a_y = \alpha_v - \alpha_h \tag{10.29}$$

i.e. the self-steering behavior depends on the difference of the slip angles between the front and rear wheels. Now, the remaining parameters can also be calculated. The yaw rate is defined as

$$\dot{\psi}_V = \frac{v}{\rho} = const, \tag{10.30}$$

the tire loads are

$$F_{v,y} = m\frac{l_h}{l}\frac{v^2}{\rho}, \quad F_{h,y} = m\frac{l_v}{l}\frac{v^2}{\rho}, \tag{10.31}$$

and the tire slip angle is (Fig. 10.7)

$$\alpha_v = \frac{F_{v,y}}{c_v} = \frac{m}{c_{\alpha,v}}\frac{l_h}{l}\frac{v^2}{\rho}, \quad \alpha_h = \frac{F_{h,y}}{c_h} = \frac{m}{c_{\alpha,h}}\frac{l_v}{l}\frac{v^2}{\rho}. \tag{10.32}$$

If a steering angle δ is applied to a vehicle driving in a straight line, then the yaw rate

$$\dot{\psi}_{V,stat} = \frac{v}{\rho} = \frac{v}{l + EG \cdot v^2}\delta_{stat} \tag{10.33}$$

has to be considered. This means that the yaw rate takes on different values depending on the self-steering gradient. One denotes

$$\frac{\dot{\psi}_V}{\delta} = \frac{v}{l + EG \cdot v^2} \tag{10.34}$$

as the yaw amplification factor for a velocity v. This factor is small for big self-steering gradients (understeering vehicle) and large for small (negative) self-steering gradients (oversteering vehicle). For

$$EG = -\frac{l}{v^2} < 0 \tag{10.35}$$

the numerator in Eq. (10.34) becomes zero and the yaw amplification factor strives toward an infinite value. In reality, this means that the vehicle will tend to become instable (more precise: it leaves the linear region), as even very small steering inputs would lead to infinite yaw rates. The velocity

$$v_{kr} = \sqrt{-\frac{l}{EG}}, \tag{10.36}$$

necessary for this to occur (consider $EG < 0$) is defined as the critical velocity. Vice versa, one can calculate the maximum yaw amplification for a given positive self-steering gradient. Through differentiation of Eq. (10.34) with respect to the velocity v one obtains:

$$\frac{d}{dv}\left(\frac{\dot{\psi}_V}{\delta}\right) = \frac{l - EG \cdot v^2}{\left(l + EG \cdot v^2\right)^2} = 0 \Rightarrow v_{ch}^2 = \frac{l}{EG}. \tag{10.37}$$

The velocity v_{ch}, at which the yaw amplification factor reaches its maximum, is called the characteristic velocity. It is interpreted as the vehicle velocity at which the vehicle reacts most sensitively to steering inputs. Typical values of v_{ch} are between 65 and 100 km/h.

10.1.3 Instationary Steering Behavior: Vehicle Stability

In order to investigate the driving stability during straight line driving, one assumes the steering angle to be equal to zero in Eq. (10.21). This way, one arrives at the linear homogenous state space equation:

$$\underbrace{\begin{bmatrix} \dot{x}_1 \\ \dot{x}_2 \end{bmatrix}}_{\dot{\boldsymbol{x}}} = \underbrace{\begin{bmatrix} -\frac{1}{v}\frac{c_{\alpha,v}l_v^2+c_{\alpha,h}l_h^2}{\theta} & -\frac{c_{\alpha,v}l_v-c_{\alpha,h}l_h}{\theta} \\ -1-\frac{1}{v^2}\frac{c_{\alpha,v}l_v-c_{\alpha,h}l_h}{m} & -\frac{1}{v}\frac{c_{\alpha,v}+c_{\alpha,h}}{m} \end{bmatrix}}_{\boldsymbol{A}} \underbrace{\begin{bmatrix} x_1 \\ x_2 \end{bmatrix}}_{\boldsymbol{x}}, \tag{10.38}$$

or in short

$$\underbrace{\begin{bmatrix} \dot{x}_1 \\ \dot{x}_2 \end{bmatrix}}_{\dot{\boldsymbol{x}}} = \underbrace{\begin{bmatrix} -\frac{1}{v}a_{11} & -a_{12} \\ -1-\frac{1}{v^2}a_{21} & -\frac{1}{v}a_{22} \end{bmatrix}}_{\boldsymbol{A}} \underbrace{\begin{bmatrix} x_1 \\ x_2 \end{bmatrix}}_{\boldsymbol{x}}, \tag{10.39}$$

with the coefficients

$$\begin{aligned} a_{11} &= \frac{c_{\alpha,v}l_v^2+c_{\alpha,h}l_h^2}{\theta}, \quad a_{12} = \frac{c_{\alpha,v}l_v-c_{\alpha,h}l_h}{\theta}, \\ a_{21} &= \frac{c_{\alpha,v}l_v-c_{\alpha,h}l_h}{m}, \quad a_{22} = \frac{c_{\alpha,v}+c_{\alpha,h}}{m}. \end{aligned} \tag{10.40}$$

As a result, one derives the polynomial for the characteristic equation of the system matrix $\boldsymbol{A}$:

$$\begin{aligned} \det(\lambda\boldsymbol{E}-\boldsymbol{A}) &= \lambda^2+\frac{1}{v}(a_{11}+a_{22})\lambda-a_{12}+\frac{1}{v^2}(a_{11}a_{22}-a_{12}a_{21}) \\ &= \lambda^2+a_1\lambda+a_2. \end{aligned} \tag{10.41}$$

The linear system (10.38) is known to be stable when both coefficients of the characteristic polynomial are positive. This is obviously always the case for a_1. From the constraint for a_2 it follows that:

$$\begin{aligned} a_2 &= -a_{12}+\frac{1}{v^2}(a_{11}a_{22}-a_{12}a_{21}) \\ &= \frac{c_{\alpha,v}c_{\alpha,h}l^2}{m\theta v^2}\left(1+\frac{c_{\alpha,h}l_h-c_{\alpha,v}l_v}{c_{\alpha,v}c_{\alpha,h}l^2}mv^2\right) > 0. \end{aligned} \tag{10.42}$$

This condition is valid for any velocity v, if:

$$c_{\alpha,h}l_h > c_{\alpha,v}l_v. \tag{10.43}$$

In any other case, the velocity is limited by following equation:

$$v^2 < \frac{1}{m}\frac{c_{\alpha,v}c_{\alpha,h}l^2}{c_{\alpha,v}l_v-c_{\alpha,h}l_h}. \tag{10.44}$$

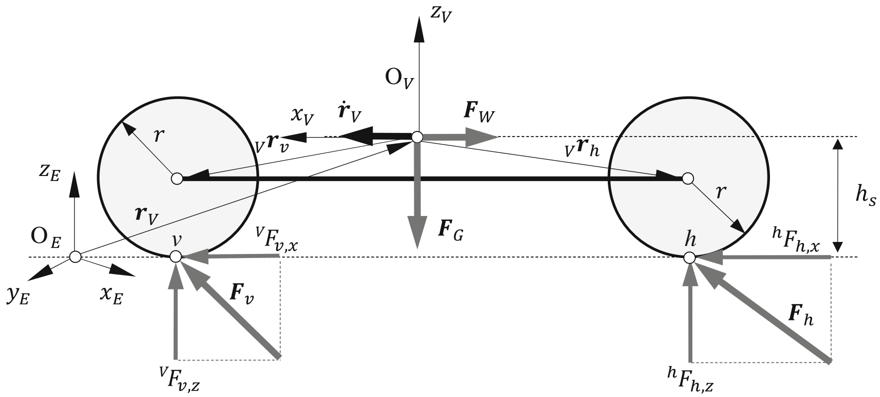

Fig. 10.8 Nonlinear single track model—*side view*

The right side of the inequality (10.44) corresponds exactly to the critical velocity v_{kr} calculated earlier. This means that an oversteering vehicle can become unstable after a certain velocity, whereas this is not the case in understeering vehicles.

10.2 Nonlinear Single Track Model

The single track model covered in the previous section already allows for a conclusive insight into the typical self-steering (eigen-) behavior of a vehicle. However, it neither includes a description of the drivetrain, nor does it allow the representation of the vehicle behavior at larger steering angles or with higher lateral accelerations. As a result, an extended model will be introduced in the following section, allowing the description of the nonlinear vehicle behavior in spite of a few restrictions.

10.2.1 Kinetics of the Nonlinear Single Track Model

The nonlinear single track model (Figs. 10.8 and 10.9) consists of

- The vehicle chassis as a rigid body, with the translational degrees of freedom x_V, y_V and the rotation ψ_V about the vertical axis.
- One imaginary front and rear wheel respectively (indices v and h), characterized by the wheel speed and tire forces.
- A given steering angle (toe angle) δ at the front axle and the steering transmission ratio i_L which are derived from the steering wheel angle δ_H as $\delta = \frac{1}{i_L}\delta_H$

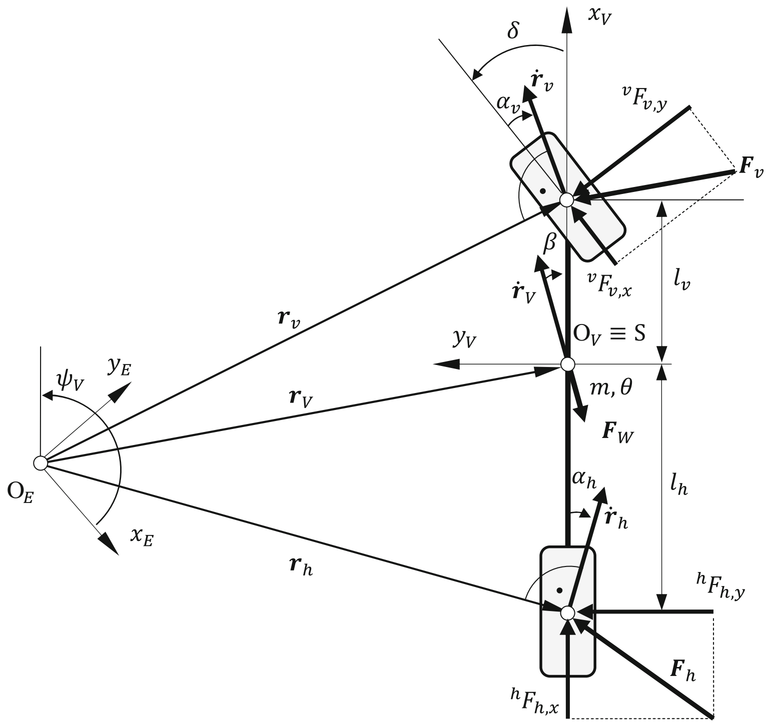

Fig. 10.9 Nonlinear single track model—*top view*

- The description of the wheel driving torques $M_{A,v}$ and $M_{A,h}$ as functions of the engine torque M_M and the current, depending on the chosen gear transmission ratio $i_G(\mathrm{G})$. The engine torque is a function of the motor rpm ω_M and the acceleration pedal position $p_F(t)$. The entire driving torque $M_A = M_{A,v} + M_{A,h}$ can be distributed arbitrarily by a factor ξ_a (also temporal) onto the front and rear axles, which allows for the simulation of a four-wheel drive configuration.
- The description of the air resistance.
- Specifying the brake torques $M_{B,v}$ and $M_{B,h}$ on the wheels as functions of the brake pedal position $p_B(t)$. The brake force distribution ξ_b can similar to ξ_a also be specified arbitrarily.

To generate the necessary equations of motion, one first applies the principle of linear momentum on the chassis, which is considered to be a rigid body:

$$m\ddot{\boldsymbol{r}}_V = \boldsymbol{F}_v + \boldsymbol{F}_h + \boldsymbol{F}_W + \boldsymbol{F}_G. \tag{10.45}$$

The acceleration of the vehicle chassis is obtained by twofold differentiation with respect to time of the position vector $\boldsymbol{r}_V$ to the center of gravity S of the vehicle given in the inertial system $\mathbf{K}_E$:

$$\boldsymbol{r}_V = \begin{bmatrix} x_V \\ y_V \\ h_S \end{bmatrix}, \dot{\boldsymbol{r}}_V = \begin{bmatrix} \dot{x}_V \\ \dot{y}_V \\ 0 \end{bmatrix}, \ddot{\boldsymbol{r}}_V = \begin{bmatrix} \ddot{x}_V \\ \ddot{y}_V \\ 0 \end{bmatrix}. \tag{10.46}$$

The forces on the front and rear wheel as well as the weights are given in coordinates of the inertial system as:

$$\boldsymbol{F}_v = \begin{bmatrix} F_{v,x} \\ F_{v,y} \\ F_{v,z} \end{bmatrix}, \quad \boldsymbol{F}_h = \begin{bmatrix} F_{h,x} \\ F_{h,y} \\ F_{h,z} \end{bmatrix}, \quad \boldsymbol{F}_G = \begin{bmatrix} 0 \\ 0 \\ -mg \end{bmatrix}. \tag{10.47}$$

As a single external force, the air resistance is given by:

$$\boldsymbol{F}_W = \frac{1}{2} c_w \rho_L A \dot{\boldsymbol{r}}_V |\dot{\boldsymbol{r}}_V| = \begin{bmatrix} F_{W,x} \\ F_{W,y} \\ 0 \end{bmatrix} = \begin{bmatrix} \frac{1}{2} c_w \rho_L A \dot{x}_V \sqrt{\dot{x}_V^2 + \dot{y}_V^2} \\ \frac{1}{2} c_w \rho_L A \dot{y}_V \sqrt{\dot{x}_V^2 + \dot{y}_V^2} \\ 0 \end{bmatrix}, \tag{10.48}$$

with an air resistance coefficient c_W, the air density ρ_L and the front surface area A of the vehicle. In this case, only the air flow opposite to the trajectory of the center of gravity of the vehicle is considered. If the influences of both the side stream and the vertical forces need to be considered, then Eq. (10.48) needs to be extended correspondingly as discussed in Chap. 9. From Eq. (10.45), and combined with the Eqs. (10.46)–(10.48), one can finally derive the complete principle of linear momentum in coordinates of the inertial system:

$$\begin{bmatrix} m\ddot{x}_V \\ m\ddot{y}_V \\ 0 \end{bmatrix} = \begin{bmatrix} F_{v,x} + F_{h,x} - F_{W,x} \\ F_{v,y} + F_{h,y} - F_{W,y} \\ F_{v,z} + F_{h,z} - mg \end{bmatrix}. \tag{10.49}$$

In a similar manner, one can arrive at the principle of angular momentum of the vehicle with respect to its center of gravity in the general form as:

$$\boldsymbol{\Theta}_V \dot{\boldsymbol{\omega}}_V + \boldsymbol{\omega}_V \times (\boldsymbol{\Theta}_V \cdot \boldsymbol{\omega}_V) = {}_V\boldsymbol{r}_v \times \boldsymbol{F}_v + {}_V\boldsymbol{r}_h \times \boldsymbol{F}_h. \tag{10.50}$$

With the moment of inertia matrix in the vehicle fixed coordinate system

$$\boldsymbol{\Theta}_V = \begin{bmatrix} 0 & 0 & 0 \\ 0 & 0 & 0 \\ 0 & 0 & \theta_{zz} \end{bmatrix}, \tag{10.51}$$

the vectors for the angular velocity and acceleration

$$ {}^{V}\boldsymbol{\omega}_V = \begin{bmatrix} 0 \\ 0 \\ \dot{\psi}_V \end{bmatrix}, \quad {}^{V}\dot{\boldsymbol{\omega}}_V = \begin{bmatrix} 0 \\ 0 \\ \ddot{\psi}_V \end{bmatrix}, \tag{10.52} $$

and the vectors for the points of application of the tire forces

$$ {}_{V}^{V}\boldsymbol{r}_v = \begin{bmatrix} l_v \\ 0 \\ -h_S \end{bmatrix}, {}_{V}^{V}\boldsymbol{r}_h = \begin{bmatrix} -l_h \\ 0 \\ -h_S \end{bmatrix}, \tag{10.53} $$

which can finally be simplified as a final vector Eq. (10.50) of the complete vehicle as a scalar equation:

$$ \theta_{zz}\ddot{\psi}_V = l_v^V F_{v,y} - l_h^V F_{h,y}. \tag{10.54} $$

10.2.2 Tire Forces

In order to evaluate the Eqs. (10.49) and (10.54), the tire forces in the wheel fixed coordinate system are required which are initially only stationary and linear with respect to cornering stiffness $c_{s,v/h}$ and $c_{\alpha,v/h}$ and the slip variables $s_{v/h}$ and $\alpha_{v/h}$:

$$ \begin{bmatrix} {}^{v}F_{v,x,stat} \\ {}^{v}F_{v,y,stat} \end{bmatrix} = \begin{bmatrix} c_{s,v}s_v \\ c_{\alpha,v}\alpha_v \end{bmatrix}, \quad \begin{bmatrix} {}^{h}F_{h,x,stat} \\ {}^{h}F_{h,y,stat} \end{bmatrix} = \begin{bmatrix} c_{s,h}s_h \\ c_{\alpha,h}\alpha_h \end{bmatrix}. \tag{10.55} $$

The force components in Eq. (10.55) later need to be included in the inertial system or the vehicle fixed system respectively. This approach is applied in Sect. 10.3, in which it shall however be considered that the four coefficients $c_{s,v}$, $c_{s,h}$, $c_{\alpha,v}$ and $c_{\alpha,h}$ are generally nonlinear and dependent on the tire loads. Alternatively to Eq. (10.55) it is also possible to use a more detailed description with a (simplified) Magic Formula (Ref. Chap. 7), especially for higher lateral accelerations, which will be dealt with below, Ref. for example (Gipser 1999; Orend 2007).

For the sake of clarity, only the definitions for the front axle are below. The corresponding definitions for the rear axle are derived simply by replacing the index "v" with "h". A simplified Magic Formula approach for the tire forces yields:

$$ \begin{bmatrix} F_{v,x,stat} \\ F_{v,y,stat} \end{bmatrix} = F_{v,z,eff} \begin{bmatrix} \mu_{v,x} \sin\left(c_{v,x} \arctan\left(b_{v,x} \frac{s_{v,a}}{\mu_{v,x}}\right)\right) \\ \mu_{v,y} \sin\left(c_{v,y} \arctan\left(b_{v,y} \frac{s_{v,a}}{\mu_{v,y}}\right)\right) \end{bmatrix}, \tag{10.56} $$

with the effective tire load

$$F_{v,z,eff} = F_{v,z}\left(1 - e_z\left(\frac{F_{v,z}}{F_{v,z,0}}\right)^2\right). \tag{10.57}$$

Equations (10.56) and (10.57) contain the friction coefficients $\mu_{v,x}$ and $\mu_{v,y}$, the tire parameters $c_{v,x}$, $c_{v,y}$, $c_{h,x}$, $c_{h,y}$ and $b_{v,x}$, $b_{v,y}$, $b_{h,x}$, $b_{h,y}$ as well as the variable tire loads ${}^{v}F_{v,z}$ and ${}^{h}F_{h,z}$. The degressive dependency of the horizontal tire forces on the tire loads is considered using the degressive parameter e_z. Furthermore, the slip variables s_v, α_v and s_h, α_h are included as the input variables for whose calculation the velocity of the wheel center point is required. This is represented by the kinematic relationships in the inertial system:

$$\begin{aligned}
\dot{\boldsymbol{r}}_v &= \dot{\boldsymbol{r}}_V + \boldsymbol{\omega}_V \times \boldsymbol{T}_V(\psi_V)\,{}^{V}_{V}\boldsymbol{r}_v \\
&= \begin{bmatrix} \dot{x}_V \\ \dot{y}_V \\ 0 \end{bmatrix} + \begin{bmatrix} 0 \\ 0 \\ \dot{\psi}_V \end{bmatrix} \times \begin{bmatrix} \cos\psi_V & -\sin\psi_V & 0 \\ \sin\psi_V & \cos\psi_V & 0 \\ 0 & 0 & 1 \end{bmatrix} \begin{bmatrix} l_v \\ 0 \\ -(h_s - r) \end{bmatrix} \\
\Rightarrow \begin{bmatrix} \dot{x}_v \\ \dot{y}_v \\ \dot{z}_v \end{bmatrix} &= \begin{bmatrix} \dot{x}_V - l_v\dot{\psi}_V \sin\psi_V \\ \dot{y}_V + l_v\dot{\psi}_V \cos\psi_V \\ 0 \end{bmatrix},
\end{aligned} \tag{10.58}$$

and

$$\begin{aligned}
\dot{\boldsymbol{r}}_h &= \dot{\boldsymbol{r}}_V + \boldsymbol{\omega}_V \times \boldsymbol{T}_V(\psi_V)\,{}^{V}_{V}\boldsymbol{r}_h \\
&= \begin{bmatrix} \dot{x}_V \\ \dot{y}_V \\ 0 \end{bmatrix} + \begin{bmatrix} 0 \\ 0 \\ \dot{\psi}_V \end{bmatrix} \times \begin{bmatrix} \cos\psi_V & -\sin\psi_V & 0 \\ \sin\psi_V & \cos\psi_V & 0 \\ 0 & 0 & 1 \end{bmatrix} \begin{bmatrix} -l_h \\ 0 \\ -(h_s - r) \end{bmatrix} \\
\Rightarrow \begin{bmatrix} \dot{x}_h \\ \dot{y}_h \\ \dot{z}_h \end{bmatrix} &= \begin{bmatrix} \dot{x}_V + l_h\dot{\psi}_V \sin\psi_V \\ \dot{y}_V - l_h\dot{\psi}_V \cos\psi_V \\ 0 \end{bmatrix}.
\end{aligned} \tag{10.59}$$

For calculating the slip values however, the velocities are required in the wheel fixed coordinate system. To this end, if one were to consider the rotation of the wheels with respect to the vehicle fixed coordinate system it would yield:

$${}^{v}\dot{\boldsymbol{r}}_v = \begin{bmatrix} {}^{v}\dot{x}_v \\ {}^{v}\dot{y}_v \\ {}^{v}\dot{z}_v \end{bmatrix} = {}^{v}\boldsymbol{T}_E \dot{\boldsymbol{r}}_v = \begin{bmatrix} \mathrm{c}(\psi_V + \delta) & \mathrm{s}(\psi_V + \delta) & 0 \\ -\mathrm{s}(\psi_V + \delta) & \mathrm{c}(\psi_V + \delta) & 0 \\ 0 & 0 & 1 \end{bmatrix} \begin{bmatrix} \dot{x}_v \\ \dot{y}_v \\ \dot{z}_v \end{bmatrix}, \tag{10.60}$$

$$ {}^{h}\dot{\boldsymbol{r}}_h = \begin{bmatrix} {}^{h}\dot{x}_h \\ {}^{h}\dot{y}_h \\ {}^{h}\dot{z}_h \end{bmatrix} = {}^{h}\boldsymbol{T}_E \dot{\boldsymbol{r}}_h = \begin{bmatrix} c\psi_V & s\psi_V & 0 \\ -s\psi_V & c\psi_V & 0 \\ 0 & 0 & 1 \end{bmatrix} \begin{bmatrix} \dot{x}_h \\ \dot{y}_h \\ \dot{z}_h \end{bmatrix}. \tag{10.61} $$

Note: In the following Eqs. (10.62)–(10.67) the tire forces are only given for the front axle. For the rear axle, the index "v" is to be replaced with the index "h". With the components of the velocity vector (10.60) and (10.61), after subtraction of the rolling velocity $r\dot{\rho}_v$ and normalizing, the longitudinal and lateral slips at the front one obtains:

$$ s_v = \frac{{}^{v}\dot{x}_v - r\dot{\rho}_v}{\max(|r\dot{\rho}_v|, |{}^{v}\dot{x}_v|)}, \tag{10.62} $$

$$ \alpha_v = -\frac{{}^{v}\dot{y}_v}{|r\dot{\rho}_v|}. \tag{10.63} $$

Now, as described in Chap. 7, the normalized total slip

$$ s_{v,a} = \sqrt{s_v^2 + \tan^2 \alpha_v} \tag{10.64} $$

is calculated at the front and rear axle. From Eq. (10.56) and the direction of action of the slip

$$ \psi_v = \arctan \frac{\alpha_v}{s_v}, \tag{10.65} $$

the resulting tire forces are given by the Eqs. (10.56)–(10.65), at first the magnitude:

$$ F_{\psi_v}(s_{v,a}) = \sqrt{\frac{s_v^2 F_{v,x,stat}^2 + \alpha_v^2 F_{v,y,stat}^2}{s_{v,a}^2}} \tag{10.66} $$

and from it, the tire forces in the wheel fixed coordinate system:

$$ \begin{bmatrix} {}^{v}F_{v,x,stat} \\ {}^{v}F_{v,y,stat} \end{bmatrix} = F_{\psi_v}\left(s_{a,v}\right) \begin{bmatrix} \cos\psi_v \\ \sin\psi_v \end{bmatrix} = \frac{1}{s_{v,a}} F_{\psi_v}\left(s_{a,v}\right) \begin{bmatrix} s_v \\ \alpha_v \end{bmatrix}. \tag{10.67} $$

To consider the settling time of the tires during fast changes of course or velocity according to Chap. 7, an addition to Eq. (10.56) is necessary. Suitable time delay constants $T_{v,x}$ and $T_{v,y}$ are chosen to represent the first order response of the system. As the conditional equation for the dynamic tire forces $\boldsymbol{F}_v$ and $\boldsymbol{F}_h$ based on the already known quasi-stationary forces $\boldsymbol{F}_{v,stat}$ and $\boldsymbol{F}_{h,stat}$ a first order differential equation is used. Exemplarily for the front axle they read:

$$\begin{bmatrix} {}^v\dot{F}_{v,x} \\ {}^v\dot{F}_{v,y} \end{bmatrix} = \begin{bmatrix} \frac{1}{T_{v,x}} & 0 \\ 0 & \frac{1}{T_{v,y}} \end{bmatrix} \left(\begin{bmatrix} {}^vF_{v,x,stat} \\ {}^vF_{v,y,stat} \end{bmatrix} - \begin{bmatrix} {}^vF_{v,x} \\ {}^vF_{v,y} \end{bmatrix} \right)$$
$$= \begin{bmatrix} \frac{c_{v,x}|r\dot{\rho}_v|}{c_{s,v}} & 0 \\ 0 & \frac{c_{v,y}|r\dot{\rho}_v|}{c_{\alpha,v}} \end{bmatrix} \left(\begin{bmatrix} {}^vF_{v,x,stat} \\ {}^vF_{v,y,stat} \end{bmatrix} - \begin{bmatrix} {}^vF_{v,x} \\ {}^vF_{v,y} \end{bmatrix} \right). \tag{10.68}$$

To this end, the time constants for the x- and y-directions are calculated according to Chap. 7 as follows:

$$\frac{1}{T_{v,x}} = \frac{c_{v,x}|r\dot{\rho}_v|}{c_{s,v}}, \quad \frac{1}{T_{v,y}} = \frac{c_{v,y}|r\dot{\rho}_v|}{c_{\alpha,v}}. \tag{10.69}$$

With the equilibrium of momentum about the vehicle center of gravity S, and the force equilibrium in the z-direction of the inertial system, the tire loads are determined. Hence, the tire normal forces at the front and the rear are:

$${}^VF_{v,z} = \frac{l_h}{l} mg - \frac{h_s}{l} \left({}^VF_{v,x} + {}^VF_{h,x} \right), \tag{10.70}$$

$${}^VF_{h,z} = \frac{l_v}{l} mg + \frac{h_s}{l} \left({}^VF_{v,x} + {}^VF_{h,x} \right). \tag{10.71}$$

Finally, the principle of momentum conservation at the front and the rear wheels with respect to the wheel center is required:

$$\theta_v \ddot{\rho}_v = M_{A,v} - \mathrm{sign}(\dot{\rho}_v) M_{B,v} - r^v F_{v,x} \tag{10.72}$$

$$\theta_h \ddot{\rho}_h = M_{A,h} - \mathrm{sign}(\dot{\rho}_h) M_{B,h} - r^h F_{h,x}. \tag{10.73}$$

10.2.3 Drive and Brake Torques

A random distribution of the driving torques between the front and the rear axle $M_{A,v}$ and $M_{A,h}$ is modeled in this example. The eigen-dynamics of the drivetrain will not be considered. For a dimensionless factor $0 \le \xi_a \le 1$, it follows:

$$M_{A,v} = (1 - \xi_a) M_A = M_A - M_{A,h}, \tag{10.74}$$

$$M_{A,h} = \xi_a M_A. \tag{10.75}$$

With this, $\xi_a = 0$ represents a front wheel drive, while $\xi_a = 1$ represents a rear wheel drive. For all other values $0 < \xi_a < 1$, a four wheel drive configuration with

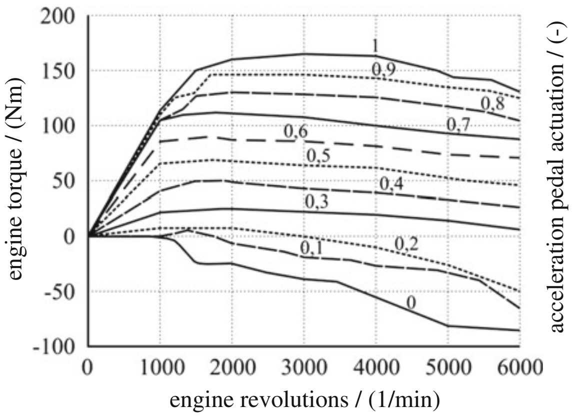

Fig. 10.10 Schematic representation of a engine characteristic curve dependent on the rpm and acceleration pedal position

variable distribution on the axles is obtained. For the calculation of the driving torque M_A one first needs an approximation of the engine speed of rotation:

$$\omega_M = i_D i_G(G)((1-\xi_a)\dot{\rho}_v + \xi_a \dot{\rho}_h), 0 \leq \xi_a \leq 1. \tag{10.76}$$

The drivetrain parameters i_D and i_G represent the transmission of the central differential and that of the gearbox respectively. In this manner, the total driving torque M_A, required for the evaluation of the Eqs. (10.72) and (10.73), based on the engine torque M_M is given by:

$$M_A = i_D i_G(G) M_M(\omega_M, p_F). \tag{10.77}$$

The engine torque is interpolated from a two dimensional engine torque characteristic curve (Fig. 10.10). Along with the engine speed ω_M, another dimensionless input parameter, the acceleration pedal position $0 \leq p_F \leq 1$ is also required. The pedal position is normally interpreted as an excitation function $p_F(t)$.

Analogous to this the brake torques are calculated as follows:

$$M_{B,v} = (1-\xi_b) M_B(p_B) = M_B(p_B) - M_{B,h}, \tag{10.78}$$

$$M_{B,h} = \xi_b M_B(p_B). \tag{10.79}$$

Here, $0 \leq \xi_b \leq 1$ is a dimensionless distribution parameter again and $p_B(t)$ is the brake pedal travel dependent on time, Ref. Fig. 10.11.

10.2.4 Equations of Motion

After the initial preliminary work in the past sections it is now possible to list the complete set of equations of motion of the nonlinear single track model.

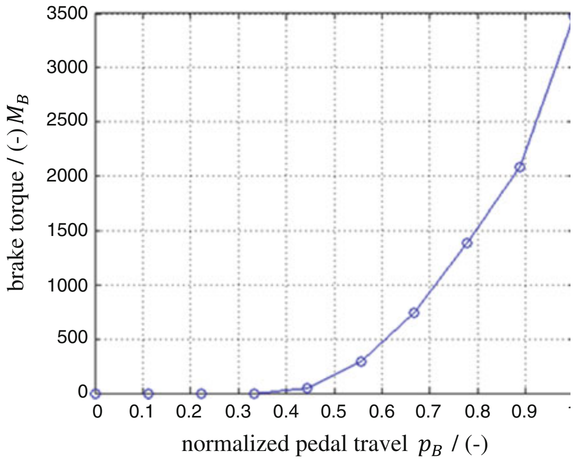

Fig. 10.11 Brake torque dependent on the brake pedal positions

- Principle of conservation of linear momentum:

$$\begin{bmatrix} m\ddot{x}_V \\ m\ddot{y}_V \end{bmatrix} = \begin{bmatrix} F_{v,x} + F_{h,x} - F_{W,x} \\ F_{v,y} + F_{h,y} - F_{W,y} \end{bmatrix}, \tag{10.80}$$

with

$$\begin{aligned} F_{W,x} &= \frac{1}{2} c_w \rho_L A \dot{x}_V \sqrt{\dot{x}_V^2 + \dot{y}_V^2}, \\ F_{W,y} &= \frac{1}{2} c_w \rho_L A \dot{y}_V \sqrt{\dot{x}_V^2 + \dot{y}_V^2}, \end{aligned} \tag{10.81}$$

$$\begin{aligned} F_{v,x} &= \cos(\psi_V + \delta)^v F_{v,x} + \sin(\psi_V + \delta)^v F_{v,y}, \\ F_{v,y} &= -\sin(\psi_V + \delta)^v F_{v,x} + \cos(\psi_V + \delta)^v F_{v,y}, \end{aligned} \tag{10.82}$$

$$\begin{aligned} F_{h,x} &= \cos\psi_V \, {}^h F_{h,x} + \sin\psi_V \, {}^h F_{h,y}, \\ F_{h,y} &= -\sin\psi_V \, {}^h F_{h,x} + \cos\psi_V \, {}^h F_{h,y}. \end{aligned} \tag{10.83}$$

- Principle of conservation of the angular momentum for the chassis in the vehicle fixed coordinate system:

$$\theta_{zz} \ddot{\psi}_V = l_v {}^V F_{v,y} - l_h {}^V F_{h,y}. \tag{10.84}$$

with

$$
\begin{aligned}
{}^{V}F_{v,y} &= \sin\delta\,{}^{v}F_{v,x} + \cos\delta\,{}^{v}F_{v,y}, \\
{}^{V}F_{h,y} &= {}^{h}F_{h,y}.
\end{aligned}
\tag{10.85}
$$

- Principle of conservation of the angular momentum for the front and rear axle:

$$\theta_v \ddot{\rho}_v = M_{A,v} - M_{B,v}\mathrm{sign}(\dot{\rho}_v) - r^v F_{v,x}, \tag{10.86}$$

$$\theta_h \ddot{\rho}_h = M_{A,h} - M_{B,h}\mathrm{sign}(\dot{\rho}_h) - r^h F_{h,x}. \tag{10.87}$$

- Dynamic tire forces:

$$\begin{bmatrix} {}^{v}\dot{F}_{v,x} \\ {}^{v}\dot{F}_{v,y} \end{bmatrix} = \begin{bmatrix} \frac{c_{v,x}|r\dot{\rho}_v|}{c_{s,v}} & 0 \\ 0 & \frac{c_{v,y}|r\dot{\rho}_v|}{c_{\alpha,v}} \end{bmatrix} \left(\begin{bmatrix} {}^{v}F_{v,x,stat} \\ {}^{v}F_{v,y,stat} \end{bmatrix} - \begin{bmatrix} {}^{v}F_{v,x} \\ {}^{v}F_{v,y} \end{bmatrix} \right), \tag{10.88}$$

$$\begin{bmatrix} {}^{h}\dot{F}_{h,x} \\ {}^{h}\dot{F}_{h,x} \end{bmatrix} = \begin{bmatrix} \frac{c_{h,x}|r\dot{\rho}_h|}{c_{s,h}} & 0 \\ 0 & \frac{c_{h,y}|r\dot{\rho}_h|}{c_{\alpha,h}} \end{bmatrix} \left(\begin{bmatrix} {}^{h}F_{h,x,stat} \\ {}^{h}F_{h,y,stat} \end{bmatrix} - \begin{bmatrix} {}^{h}F_{h,x} \\ {}^{h}F_{h,y} \end{bmatrix} \right). \tag{10.89}$$

10.2.5 Equations of State

One can now transfer the equations of motion into the state space form:

$$\dot{\boldsymbol{x}} = \boldsymbol{f}(\boldsymbol{x}, t, \boldsymbol{u}), \tag{10.90}$$

with the state vector

$$\boldsymbol{x} = \left[x_V, y_V, \psi_V, \dot{x}_V, \dot{y}_V, \dot{\psi}_V, \dot{\rho}_v, \dot{\rho}_h, {}^{v}F_{v,x}, {}^{v}F_{v,y}, {}^{h}F_{h,x}, {}^{h}F_{h,y} \right]^T \tag{10.91}$$

and the excitation vector

$$\boldsymbol{u} = [\delta_H, p_F, p_B, G]^T. \tag{10.92}$$

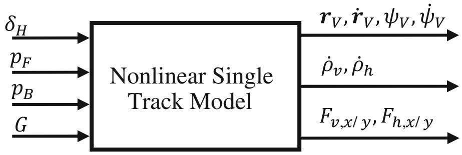

Fig. 10.12 Nonlinear single track model of a dynamic system

Along with the acceleration and brake pedal position p_F and p_B, the steering wheel angle δ_H and the gear parameter G (defining the gear engaged) also appear. As a result, the nonlinear single track model can be represented as a dynamic system as shown in Fig. 10.12.

As a whole, the Eqs. (10.90)–(10.92) read:

$$\underbrace{\begin{bmatrix} \dot{x}_V \\ \dot{y}_V \\ \dot{\psi}_V \\ \ddot{x}_V \\ \ddot{y}_V \\ \ddot{\psi}_V \\ \ddot{\rho}_v \\ \ddot{\rho}_h \\ {}^V\dot{F}_{v,x} \\ {}^V\dot{F}_{v,y} \\ {}^V\dot{F}_{h,x} \\ {}^V\dot{F}_{h,y} \end{bmatrix}}_{\dot{\boldsymbol{x}}} = \underbrace{\begin{bmatrix} \dot{x}_V \\ \dot{y}_V \\ \dot{\psi}_V \\ \frac{1}{m}(F_{v,x} + F_{h,x} - F_{W,x}) \\ \frac{1}{m}(F_{v,y} + F_{h,y} - F_{W,y}) \\ \frac{1}{\theta_{zz}}(l_v {}^V F_{v,y} - l_h {}^V F_{h,y}) \\ \frac{1}{\theta_v}(M_{A,v} - M_{B,v}\mathrm{sign}(\dot{\rho}_v) - r\, {}^vF_{v,x}) \\ \frac{1}{\theta_h}(M_{A,h} - M_{B,h}\mathrm{sign}(\dot{\rho}_h) - r\, {}^hF_{h,x}) \\ \frac{c_{v,x}|r\dot{\rho}_v|}{c_{s,v}}\left({}^vF_{v,x,stat} - {}^vF_{v,x}\right) \\ \frac{c_{v,y}|r\dot{\rho}_v|}{c_{\alpha,v}}\left({}^vF_{v,y,stat} - {}^vF_{v,y}\right) \\ \frac{c_{h,x}|r\dot{\rho}_h|}{c_{s,h}}\left({}^hF_{h,x,stat} - {}^hF_{h,x}\right) \\ \frac{c_{h,y}|r\dot{\rho}_h|}{c_{\alpha,h}}\left({}^hF_{h,y,stat} - {}^hF_{h,y}\right) \end{bmatrix}}_{\boldsymbol{f}(\boldsymbol{x},t,\boldsymbol{u})} \tag{10.93}$$

10.3 Linear Roll Model

Due to their modeling constraints, the single track models discussed in this chapter so far do not allow the description and investigation of effects resulting from different tire loading, for example during cornering. These effects will obviously be included in the spatial modeling, which is the focus of Chaps. 11 and 12. It is however also possible for real time simulations or for simple fundamental investigations in example, to model and consider such effects in the single track models discussed until now. However, the following constraints still hold:

- Changes in the chassis geometry as a result of the forces will not be considered. This means that all equilibrium conditions need to be formulated from the output geometry.

http://www.springer.com/978-3-540-36044-5

Vehicle Dynamics
Modeling and Simulation
Schramm, D.; Hiller, M.; Bardini, R.
2014, XIX, 405 p. 327 illus., Hardcover
ISBN: 978-3-540-36044-5